ISIJ International, Vol. 48 (2008), No. 9, pp. 1197–1205

Development of a Decarburization and Slag Formation Model for the Electric Arc Furnace

Hiroyuki MATSUURA,[1] Christopher P. MANNING,[2] Raimundo A. F. O. FORTES[3] and Richard J. FRUEHAN[4]

1) Formerly Center for Iron and Steelmaking Research, Department of Materials Science and Engineering, Carnegie Mellon University. Now at Department of Advanced Materials Science, Graduate School of Frontier Sciences, The University of Tokyo, 5-1-5 Kashiwanoha, Kashiwa, Chiba 277-8561 Japan. 2) Materials Processing Solutions, Inc., PO Box 1203, Easton, MA 02334 U.S.A. 3) Department of Technology and Industrial Process, Gerdau Aços Longos Brasil S.A., Av. Joao XXIII, 6777-Distrito Industrial Santa Cruz, Rio de Janeiro RJ 23560-900 Brazil.
4) Center for Iron and Steelmaking Research, Department of Materials Science and Engineering, Carnegie Mellon University, 5000 Forbes Avenue, Pittsburgh, PA 15213 U.S.A.

(*Received on March 6, 2008; accepted on June 9, 2008*)

A decarburization and slag formation model for the electric arc furnace was developed, which includes the rate phenomena for decarburization and the reaction between carbonaceous materials and iron oxide in slag, mass balance for each species in the metal, slag and gas phases, and the melting behavior of pig iron, scrap and fluxes. The model was applied to a two bucket charge operation electric arc furnace and the dynamic metal and slag compositions were calculated as a function of time. The effects of melting patterns for raw materials, carbon–FeO reaction rate, and the post combustion ratio were examined. The critical parameters, which most strongly influence chemistry development, were identified. These parameters were fitted to an industrial case, such that the model could accurately predict slag and metal chemistry development. This model could be utilized to optimize the operation in order to improve yield, energy efficiency, and increase consistency of metal and slag chemistries from heat to heat.

KEY WORDS: electric arc furnace; decarburization; slag formation; mass balance; model development.

1. Introduction

Electric arc furnace (EAF) production of steel has grown significantly in the past several decades. Much of this production is in state of the art plants producing higher value added products such as continuously cast flat rolled steels. These furnaces use large quantities of pig iron, injected oxygen, and injected carbon for foamy slag[1] and electrical energy. Injected oxygen can react directly with iron to form iron oxide, carbon dissolved in iron or solid carbon to form CO, or with CO in the gas phase in the form of post combustion producing CO_2. How the oxygen is distributed among these reactions is critical to the furnace performance.

In the present study, a decarburization and slag formation model has been developed based on a mass balance, and the kinetic equations for decarburization, and the reduction reaction between carbonaceous materials and iron oxide in slag. Various melting patterns for scrap and pig iron were examined and the variations of carbon content in the metal and iron oxide content in slag were calculated. The model developed here can be used to optimize oxygen injection, flux additions, carbon injection, and yield as well as slag foaming, which is the subject of a future paper.

Several successful models have been developed for oxygen steelmaking (OSM).[2] OSM is a true batch process in which all of the hot metal, scrap and fluxes are added before the oxygen blow begins, and all of the metal and slag are tapped at the end of the process. The major part of an OSM vessel charge, liquid hot metal, is homogenous in temperature, physical properties and chemistry. Many modern EAFs operate with a liquid heel of metal and slag from the previous heat, flux and carbon are injected continuously during various stages of the process, and slag is flushed out of the furnace. Furthermore, injected carbon reduces FeO dissolved in the slag throughout the heat. In addition, the entire charge of an EAF is solid scrap, and extremely heterogeneous with respect to chemistry, bulk density, and other physical parameters. In the EAF, decarburization is controlled by liquid phase mass transfer at low carbon content, which this paper will demonstrate is true for much of the EAF melting cycle. These considerations make a model for the EAF much more complicated than for the OSM process. Several previous models have been developed, such as energy and materials balances for charge control and for FeO formation.[2] However, no comprehensive model exists, which takes into account the many dynamic effects and reaction rates.

2. Model Development

The present decarburization and slag formation model is based a mass balance for each component in metal and slag phases, and the rate equations for decarburization and the

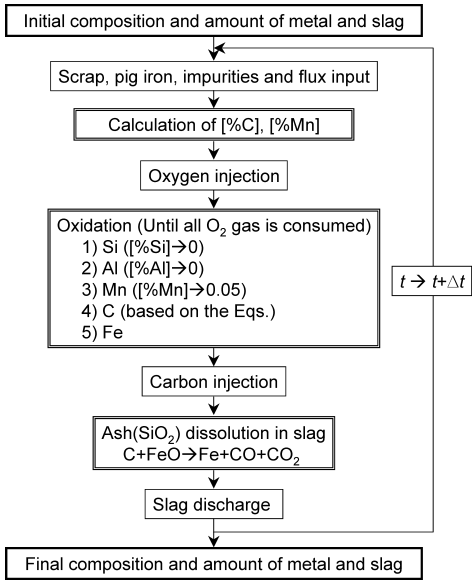

Fig. 1. Calculation algorithm in the present model.

reduction of iron oxide in slag by injected carbonaceous materials. **Figure 1** shows the model calculation algorithm chart. The calculation algorithm is mainly composed of (A) melting of scrap and pig iron, and dissolution of impurities associated with scrap, such as dirt, and flux, (B) oxidation of carbon and other elements including iron by injected oxygen, (C) reduction of iron oxide by injected carbonaceous materials, (D) slag discharge or flushing, and (E) mass balance calculations. Steps (A) to (E) were repeated until the end of the refining by the time step of Δt.

(A) Scrap and Pig Iron Melting, and Impurity and Flux Dissolution

Scrap, pig iron and the accompanying impurities are melted or dissolved into slag, and included in metal and slag phases based on the defined (assumed) melting or dissolution rate. If flux is injected during refining, this also is taken into consideration. Metal and slag phases are assumed to be homogeneous, and then compositions of each element in metal and slag phases are calculated.

(B) Oxidation of Carbon and Other Elements by Oxygen

Injected oxygen first oxidizes elements more easily oxidized than carbon and iron. In the present model, as the scrap melts the silicon, aluminum and manganese are oxidized until their compositions reach the set points of each element. In the present calculation, it was assumed that silicon and aluminum in melt are completely oxidized, and manganese is oxidized until manganese content reaches 0.05 mass%.

$$\underline{Si}+O_2\,(g)=(SiO_2) \quad \text{.....(1)}$$

$$\underline{Al}+3/4\,O_2\,(g)=1/2\,(Al_2O_3) \quad \text{.....(2)}$$

$$\underline{Mn}+1/2\,O_2\,(g)=(MnO) \quad \text{.....(3)}$$

The SiO_2, Al_2O_3 and MnO produced enter into the slag phase.

Second, decarburization proceeds by Eq. (4) as in OSM.[3] It is well accepted that the reaction proceeds by oxygen first reacting with iron to form FeO in slag. Then carbon diffuses in the metal reducing the FeO to metallic iron and producing CO as indicated by the following reactions.

$$\underline{C}+1/2\,O_2\,(g)=CO\,(g) \quad \text{.....(4)}$$

$$\underline{Fe}+1/2\,O_2\,(g)=(FeO) \quad \text{.....(5)}$$

$$(FeO)+\underline{C}=\underline{Fe}+CO\,(g) \quad \text{.....(6)}$$

The CO can be further oxidized to CO_2 by post combustion.

If the carbon content is high, the driving force for mass transfer of carbon is sufficient to reduce all of the FeO formed. As a result, the rate of decarburization is limited by the oxygen mass flow rate. At low carbon contents, the mass transfer rate decreases and not all of the FeO is reduced, thus the FeO content of the slag increases. Therefore, the decarburization rate is controlled by liquid phase mass transfer of carbon at lower carbon content as expressed by Eq. (7), or by oxygen gas flow rate at higher carbon content described by Eq. (8).

$$\frac{d[\%C]_t}{dt}=-\frac{mA\rho}{W_t^{Melt}}([\%C]_t-[\%C]_t^e) \quad \text{.....(7)}$$

$$\frac{d[\%C]_t}{dt}=-\frac{V_t^{Oxy}\times 1\,000/22.4\times(2-R_{PC})\times 0.012}{W_t^{Melt}}\times 100 \quad \text{.....(8)}$$

where, m is the liquid phase mass transfer coefficient of carbon, A is the interfacial area where the decarburization occurs, ρ is the density of melt, W_t^{Melt} is the weight of metal phase at time is t, V_t^{Oxy} is the oxygen gas injection rate at time is t, and R_{PC} is the post combustion ratio. Since the equilibrium carbon content $[\%C]^e$ is negligibly small compared to carbon content in melt, $[\%C]^e$ was assumed to be zero. The point where the rate mechanism changes is called the critical carbon content $[\%C]^C$.

The value of "mA" is normally obtained by measuring the rate of decarburization in the furnace and back calculating the parameter using Eq. (7). However, due to the heterogeneous distribution of solid and liquid in an EAF during melting, it is nearly impossible to get a representative liquid metal sample during the first half of the oxygen injection period. As a result, no measurements are available for an EAF. In the present work, the value of "mA" was extrapolated from OSM operations assuming the parameter is proportional to the oxygen flow rate. This assumption is valid in OSM, as the stirring energy in the bath is typically proportional to the oxygen injection rate. Since the value of mA/V^{Oxy} depends on many factors such as the furnace size, shape, O_2 injection method and so on, the intrinsic value should be known to calculate the decarburization rate in the particular furnace accurately. In the present calculation, the value of mA/V^{Oxy} used in this study was 0.050 which value is reported for 300 t vessel[4] based on the above assumption and the critical carbon content was calculated by equating Eqs. (7) and (8), and is approximately 0.3 mass%.[3,4]

When the carbon content decreases below the critical value, the oxidation reaction of iron becomes dominant, and iron oxide is produced, which is absorbed by the slag phase. The reactions between decarburization and iron oxidation are competitive, and the proportion between these two reactions is determined by the carbon content as de-

scribed by Eqs. (7) and (8). The amount of FeO in the slag is determined from the oxygen injected minus any oxygen used for carbon burning, post combustion and the oxidation of alloying elements (Al, Si, Mn) in the scrap. In the EAF, part of oxygen reacts directly with the solid scrap producing FeO, and as the scrap melts, the FeO on the scrap reports to the slag phase. However, the calculated FeO formed in the model is based on a mass balance in which the oxygen not used for carbon, CO, or elements in the metal oxidizes iron. Therefore, the formation of FeO by the reaction of oxygen with scrap is accounted for, though not explicitly calculated.

(C) Reduction of Iron Oxide by Injected Carbonaceous Materials

During EAF steelmaking, carbonaceous materials such as coke and coal are injected into the slag to reduce iron oxide in slag phase and make the slag foam. Slag foaming is critical for the protection of refractories and the water cooled roof and sidewalls from the arc, as well as, to minimize the heat loss. However, it is frequently observed that the some injected carbon remains in slag and is discharged as unreacted particles. It was assumed that the reduction rate of iron oxide by carbon particles is expressed as Eq. (9). This equation assumes that the rate is controlled by mass transfer of FeO in the slag or chemical kinetics and the surface area of carbon is proportional to its weight in the slag.

$$r_t^{\mathrm{red}} = k_{\mathrm{red}} \cdot W_t^{\mathrm{CM}} \cdot \frac{(\%\mathrm{FeO})_t}{100} \quad \text{.....(9)}$$

where, k_{red} is the reaction rate constant between carbon and iron oxide in slag, and W_t^{CM} is the weight of carbon existing in slag at time is t. In this model, the reduced iron returns to the metal phase. In the present calculations, k_{red} is considered as a constant value throughout the refining time. On the other hand, k_{red} is obviously a function of temperature and temperature profile of the metal and slag during the operation should be considered to determine k_{red} more exactly. However, change of temperature is not calculated in this model and other calculation (estimation) model should be utilized to estimate temperature in the future step. In addition, the optimized k_{red} calculated in the present application is $0.57\,\mathrm{min}^{-1}$ as discussed in the following section. Though an increased k_{red} of $1.5\,\mathrm{min}^{-1}$ (corresponding to the activation energy of 282 kJ/mol in the case of temperature change from 1 823 to 1 923 K) was examined in the case study, carbon content profile in metal did not change and the difference in FeO content profile by the use of two k_{red} values was only within 2.5 mass%. Therefore, the effect of temperature change in the present calculation is limited.

(D) Slag Discharge

During EAF steelmaking, slag is discharged or flushed during the process. Assuming that the slag phase is homogeneous, part of the slag is discharged according to a defined slag discharge rate. Unreacted carbon remaining in slag is also discharged with the slag.

(E) Mass Balance Calculations

The mass balance calculations in metal and slag phases are expressed by following equations. In the present model, the refractory dissolution has not been included for the slag mass balance calculation. It will be incorporated in the further model development. The refractory consumption in different EAF operations varies greatly, and can be between 0.2–2.0 kg/t-metal.[5] At present, the model assumes the increase of MgO content in the slag is expected to be minor.

[Metal phase]

$$W_t^{\mathrm{Melt}} = W_t^{\mathrm{Fe}} + W_t^{\mathrm{C}} + W_t^{\mathrm{Mn}} + W_t^{\mathrm{Si}} + W_t^{\mathrm{Al}} \quad \text{.....(10)}$$

$$W_{t+\Delta t}^{\mathrm{Fe}} = W_t^{\mathrm{Fe}} + (r_t^{\mathrm{Pig}} \cdot C_{\mathrm{Pig}}^{\mathrm{Fe}} + r_t^{\mathrm{Scrap}} \cdot C_{\mathrm{Scrap}}^{\mathrm{Fe}}) \cdot \Delta t - W_t^{\mathrm{Fe\text{-}Oxi}} + W_t^{\mathrm{Fe\text{-}Red}} \quad \text{.....(11)}$$

$$W_{t+\Delta t}^{\mathrm{C}} = W_t^{\mathrm{C}} + (r_t^{\mathrm{Pig}} \cdot C_{\mathrm{Pig}}^{\mathrm{C}} + r_t^{\mathrm{Scrap}} \cdot C_{\mathrm{Scrap}}^{\mathrm{C}}) \cdot \Delta t - W_t^{\mathrm{C\text{-}Oxi}} \quad \text{.....(12)}$$

$$W_{t+\Delta t}^{\mathrm{Mn}} = W_t^{\mathrm{Mn}} + (r_t^{\mathrm{Pig}} \cdot C_{\mathrm{Pig}}^{\mathrm{Mn}} + r_t^{\mathrm{Scrap}} \cdot C_{\mathrm{Scrap}}^{\mathrm{Mn}}) \cdot \Delta t - W_t^{\mathrm{Mn\text{-}Oxi}} \quad \text{.....(13)}$$

$$W_{t+\Delta t}^{\mathrm{Si}} = W_t^{\mathrm{Si}} + (r_t^{\mathrm{Pig}} \cdot C_{\mathrm{Pig}}^{\mathrm{Si}} + r_t^{\mathrm{Scrap}} \cdot C_{\mathrm{Scrap}}^{\mathrm{Si}}) \cdot \Delta t - W_t^{\mathrm{Si\text{-}Oxi}} \quad \text{.....(14)}$$

$$W_{t+\Delta t}^{\mathrm{Al}} = W_t^{\mathrm{Al}} + r_t^{\mathrm{Scrap}} \cdot C_{\mathrm{Scrap}}^{\mathrm{Al}} \cdot \Delta t - W_t^{\mathrm{Al\text{-}Oxi}} \quad \text{.....(15)}$$

[Slag phase]

$$W_{t'}^{\mathrm{FeO}} = W_t^{\mathrm{FeO}} + (W_t^{\mathrm{Fe\text{-}Oxi}} - W_t^{\mathrm{Fe\text{-}Red}}) \cdot \frac{72}{56} \quad \text{.....(16)}$$

$$W_{t'}^{\mathrm{CaO}} = W_t^{\mathrm{CaO}} + (r_t^{\mathrm{Flux}} \cdot C_{\mathrm{Flux}}^{\mathrm{CaO}} + r_t^{\mathrm{Dirt}} \cdot C_{\mathrm{Dirt}}^{\mathrm{CaO}}) \cdot \Delta t \quad \text{.....(17)}$$

$$W_{t'}^{\mathrm{SiO_2}} = W_t^{\mathrm{SiO_2}} + (r_t^{\mathrm{Dirt}} \cdot C_{\mathrm{Dirt}}^{\mathrm{SiO_2}} + r_t^{\mathrm{CM}} \cdot C_{\mathrm{CM}}^{\mathrm{SiO_2}}) \cdot \Delta t + W_t^{\mathrm{Si\text{-}Oxi}} \cdot \frac{60}{28} \quad \text{.....(18)}$$

$$W_{t'}^{\mathrm{MgO}} = W_t^{\mathrm{MgO}} + (r_t^{\mathrm{Flux}} \cdot C_{\mathrm{Flux}}^{\mathrm{MgO}} + r_t^{\mathrm{Dirt}} \cdot C_{\mathrm{Dirt}}^{\mathrm{MgO}}) \cdot \Delta t \quad \text{...(19)}$$

$$W_{t'}^{\mathrm{Al_2O_3}} = W_t^{\mathrm{Al_2O_3}} + r_t^{\mathrm{Dirt}} \cdot C_{\mathrm{Dirt}}^{\mathrm{Al_2O_3}} \cdot \Delta t + W_t^{\mathrm{Al\text{-}Oxi}} \cdot \frac{51}{27} \quad \text{...(20)}$$

$$W_{t'}^{\mathrm{MnO}} = W_t^{\mathrm{MnO}} + W_t^{\mathrm{Mn\text{-}Oxi}} \cdot \frac{71}{55} \quad \text{.....(21)}$$

$$W_t^{\mathrm{Slag}} = \sum W_t^{\mathrm{MeO}_n} \quad \text{.....(22)}$$

$$C_{t+\Delta t}^{\mathrm{MeO}_n} = \frac{W_{t'}^{\mathrm{MeO}_n}}{W_{t'}^{\mathrm{Slag}}} \quad \text{.....(23)}$$

$$W_{t+\Delta t}^{\mathrm{MeO}_n} = (W_{t'}^{\mathrm{Slag}} - r_t^{\mathrm{Dis}} \cdot \Delta t) \cdot C_{t+\Delta t}^{\mathrm{MeO}_n} \quad \text{.....(24)}$$

A number of other factors are important and primarily depend on the specific operation. For example dust losses are not considered. As discussed latter up to 10 kg/t-scrap of iron or more leaves the furnace as dust. Post combustion depends on the actual operation. In this model it is an input and usually assumed to be 10%. As mentioned above, refractory dissolution will also affect the chemistry and amount of slag.

3. Application of the Model

In the present study, the model developed was applied to a two bucket charge operation furnace. **Table 1** shows typical operational conditions and raw materials for this fur-

nace. In this model, the calculated results are obtained by integrating calculated values with a time interval of Δt. Effect of Δt on the calculation results was preliminary examined and sufficiently small value of $\Delta t = 1/60$ min (1.0 s) was selected as a calculation condition.

The furnace is a 120 t capacity with a 105 t tap weight. Scrap and pig iron are charged in two buckets. Dolomite and lime are charged with the scrap and pig iron in the first bucket. In the latter stage of the refining, coke is injected for foaming and FeO reduction, and slag is discharged from the furnace.

Table 1. Operational conditions, the raw materials and calculation conditions.

Liquid Steel Capacity	120 t	
Tapping	105 t	
Operation time	50 min	
First bucket	Before operation	
Second bucket	10 min	
Raw materials	Amount	(mass%)
Pig iron	48400 kg	
- Metal	47916 kg (99.0 %)	Fe: 95.6 C: 4.2 Si: 0.1 Mn: 0.1
- Impurity	484 kg (1.0 %)	CaO: 15 MgO: 10 Al_2O_3: 15 SiO_2: 60
Scrap	67200 kg	
- Metal	64848 kg (96.5 %)	Fe:99.0 C: 0.2 Si: 0.1 Mn: 0.7
- Impurity	2352 kg (3.5 %)	CaO: 15 MgO: 10 Al_2O_3: 15 SiO_2: 60
Flux		
- Dolomite	1490 kg (Initial charge)	CaO: 56.43 MgO: 40.57
- Lime	2387 kg (Initial charge)	CaO: 95 SiO_2: 2
Coke injection	877 kg (20.5-50.0 min)	C_{fixed}: 90 SiO_2: 5
Electrode	130 kg (12.0-50.0 min)	C_{fixed}: 100
Oxygen injection	4212 Nm^3 Rate varies in process	
Initial heel		
Metal	15000 kg	
Slag	6000 kg	
Slag discharge	11000 kg (41.0-50.0 min)	
Δt	1/60 min (1.0 s)	

3.1. Effect of Materials Melting Pattern

The effect of the pig iron and scrap melting rates were examined for the furnace. The oxygen injection rate varies with time, reflecting oxygen injection in the actual process. Since the furnace is operated with a two bucket charge, there is an idle time between 5 and 13 min after the start of the operation for the second bucket charge. During the idle time the oxygen flow rate is very low. There are two types of oxygen injectors; the main lances for refining of melt, and secondary injectors for the post combustion. In the present calculation, post combustion occurring above the melt and slag phases are not taken into account, because this does not affect the melt and slag chemistries. Therefore, it was assumed that 100% of main lance oxygen and 20% of post combustion oxygen reacts with the melt and slag based on discussions with furnace operators. It was also assumed that the scrap impurities and charged flux in the first bucket dissolve in slag with a constant dissolution rate in the first 30 min. The reaction rate constant between FeO and carbon particles in slag k_{red} and the post combustion ratio R_{PC} were fixed to be 1.0 min^{-1} and 0.1, respectively. Four pig iron melting patterns and three scrap melting patterns were defined (assumed) as shown in **Fig. 2** based on discussions with the furnace operators and the fundamental considerations. In the calculations, the final metal and slag chemistries were used as the initial condition of the metal and slag heel for the next calculation, and this procedure was repeated several times until the steady state results were obtained.

Figure 3 shows the change of carbon content in melt as a function of time for each melting pattern, together with the analytical results of collected melt samples. The furnace has only 15 000 kg of initial heel compared to 115 600 kg of charged materials. Therefore, the carbon content in the melt changes considerably with different melting patterns of pig iron and scrap. Assuming a fast melting rate for pig iron at the early stage of operation, the carbon content goes up to 0.7 mass%. For all melting patterns, stable carbon content profiles were seen after about 30 min. However, those were approximately 0.1–0.25 mass%, which is higher than the observed carbon content in the furnace of about 0.06 mass%.

Figure 4 shows the change of FeO content in slag as a function of time for each melting pattern with the analytical

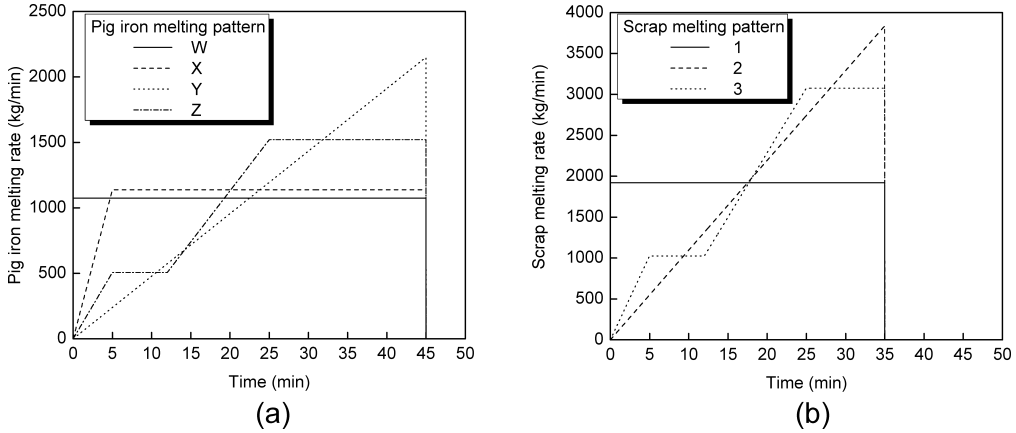

Fig. 2. Defined melting patterns for (a) pig iron and (b) scrap.

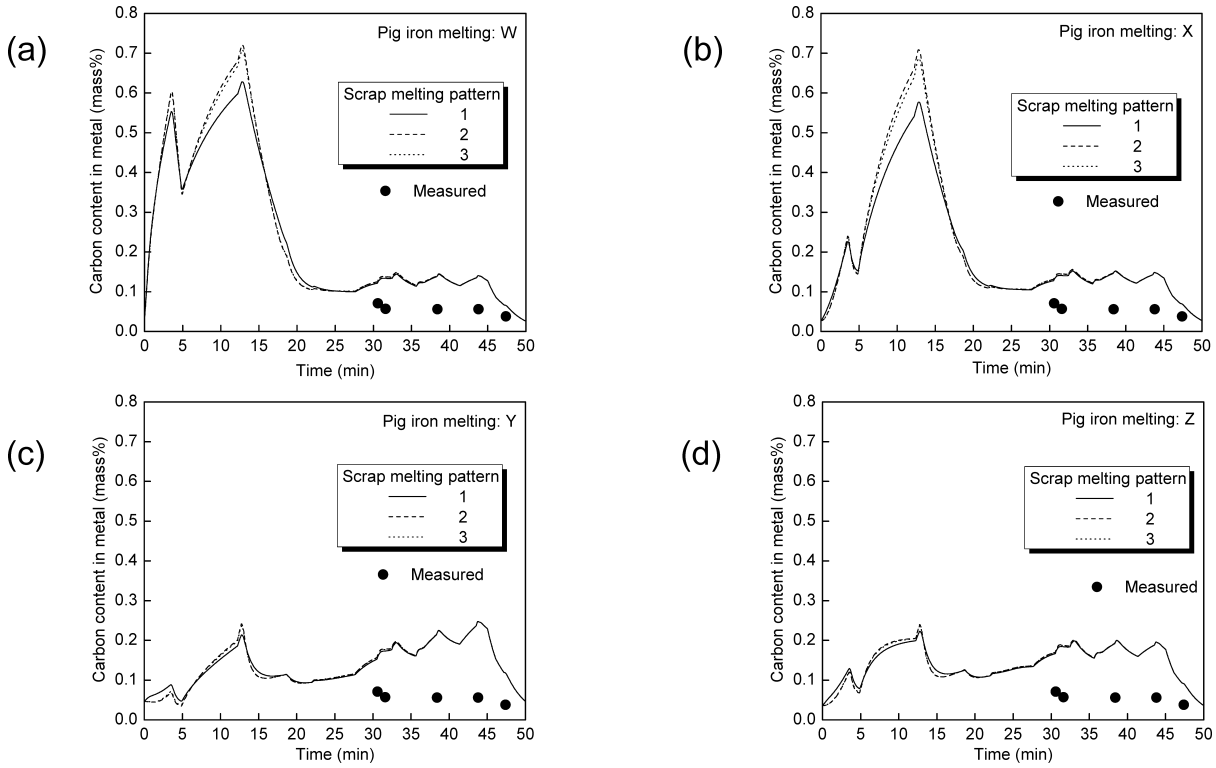

Fig. 3. Change of carbon content in the melt calculated with various pig iron and scrap melting patterns.

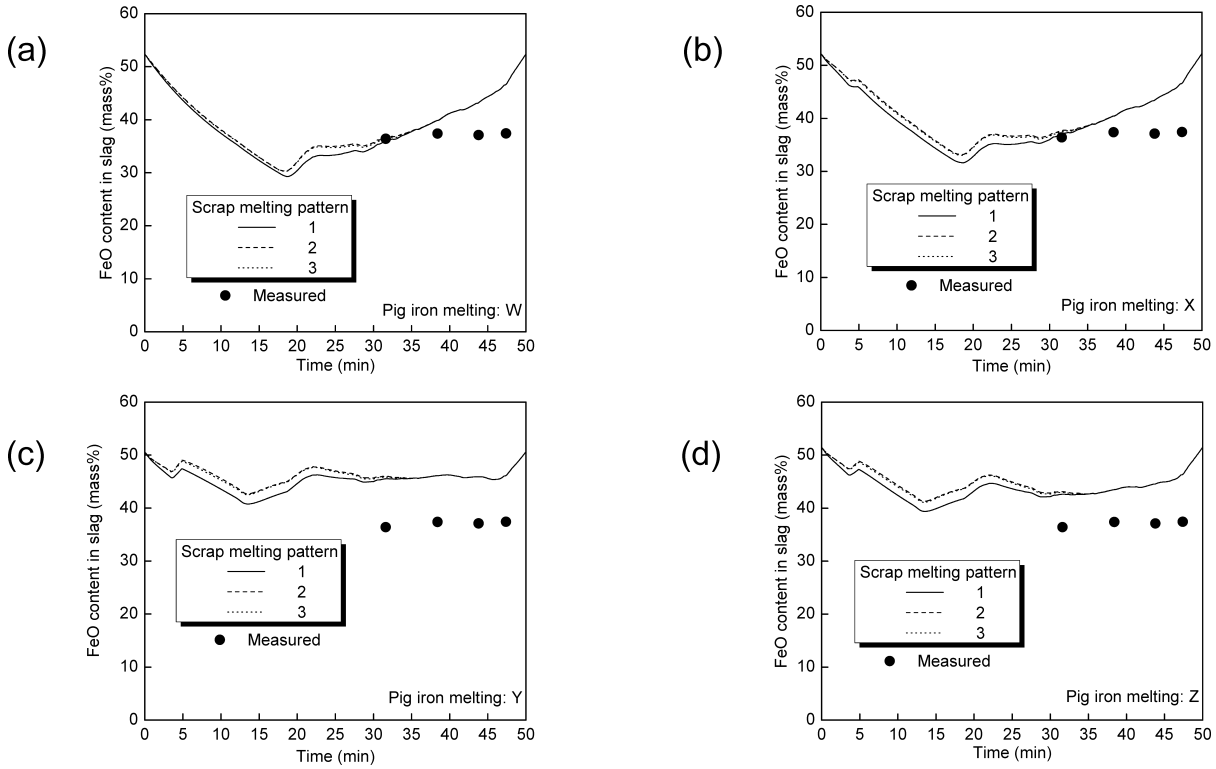

Fig. 4. Change of FeO content in slag calculated with various pig iron and scrap melting patterns.

results of collected slag samples. The minimum FeO content was calculated to occur between 10 and 20 min. Then the FeO content increased again or remained almost constant. Faster melting of pig iron in the early stage, such as patterns W and X for pig iron melting, leads to a large decrease in FeO content. This is because the carbon content in the melt increases, and all oxygen injected is consumed by the decarburization reaction and no FeO is produced, while the scrap impurities and fluxes dissolve continuously causing the FeO to be diluted. In the early stage of the operation, some FeO should be produced and supplied to the slag phase to enhance the flux dissolution and maintain FeO level. On the other hand, in the case of patterns Y and Z for pig iron melting, the FeO content was almost constant dur-

Table 2. Calculated FeO and carbon loss for each melting pattern (unit: kg).

	[Pig iron]							
	W		X		Y		Z	
[Scrap]	FeO	Carbon	FeO	Carbon	FeO	Carbon	FeO	Carbon
1	5003	5.43	5012	5.40	5124	5.13	5063	5.27
2	5003	5.43	5012	5.40	5124	5.13	5063	5.27
3	5003	5.43	5012	5.40	5124	5.13	5063	5.27

ing the operation. Considering the change of carbon and FeO contents with time, slower melting of pig iron in the early stage, for example patterns Y and Z, would be realistic for this furnace. However, the calculated FeO content was higher compared to the analyzed results by about 5–10 mass% as shown in Fig. 4. The overestimated FeO content would be due to (i) the overestimation of the contribution of the injected oxygen from the post combustion injectors to the reaction and (ii) the underestimated post combustion ratio.

The calculated FeO and carbon loss by slag discharge are shown in **Table 2** for each melting pattern of pig iron and scrap. The FeO and carbon loss changes with pig iron melting pattern, while the effect of scrap melting pattern is small. The carbon loss with the slag discharge is 0.6%.

Considering effect of melting patterns for pig iron on the profile of carbon content in metal and FeO content in slag, pig iron melting pattern Z seems most realistic one. The optimization of pig iron melting pattern should be conducted together with other operational variables to reproduce the operational results. In the following calculations, pig iron melting pattern Z was used as a most conceivable pattern for the time being to examine other parameters. On the other hand, "the ideal melting pattern" of pig iron for a particular furnace to operate the furnace at the best condition can be obtained from this model with other tuned parameters.

3.2. Effect of Carbon–FeO Reaction Rate Constant

The effect of the reaction rate constant k_{red} was examined with fixed pig iron and scrap melting patterns (Z and 3, respectively). The post combustion ratio was assumed to be 0.1. Change of the reaction rate constant k_{red} does not affect carbon content in metal considerably (within 0.008 mass%), though FeO content changes. **Figure 5** shows the FeO content profiles in slag with various carbon–FeO reaction rate constants at steady state. Decreasing the rate constant increases FeO content in slag and, as a result, FeO and carbon loss also increase. The loss of FeO and unreacted carbon with various reaction rate constants are shown in **Table 3**. The value of the reaction rate constant is between 0.1 and 0.5 min^{-1} to reach 10% of carbon loss. In the case of 0.5 min^{-1}, the calculated FeO level was approximately 10 mass% above the analyzed slag composition.

3.3. Effect of Post Combustion Ratio

The effect of post combustion ratio on FeO content was examined with fixed pig iron and scrap melting patterns (Z and 3, respectively) and carbon–FeO reaction rate constant (0.5 min^{-1}). **Figure 6** shows the FeO content profiles in the slag with three post combustion ratios at steady state. When the post combustion ratio is increased to $R_{PC}=0.3$, the FeO content in the slag decreases or remains constant reproducing the analyzed slag chemistry after 30 min. The large increase of FeO content after 45 min is due to the termination of pig iron melting, resulting in an FeO content in slag at the end of the heat of 40–45 mass%.

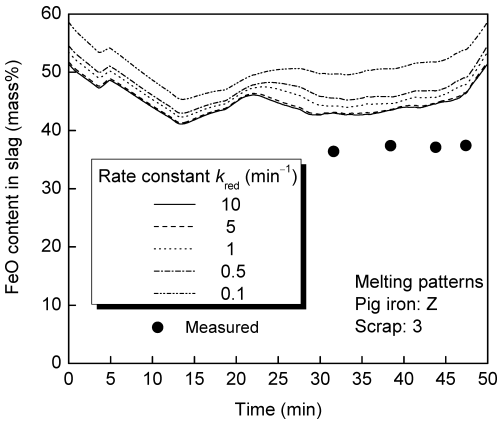

Fig. 5. Change of FeO content in slag with changing carbon–FeO reaction rate constant k_{red}.

Table 3. Calculated FeO and carbon loss with various carbon–FeO reaction rate constants with fixed pig iron and scrap melting patterns.

	Reaction rate constant k_{red} (min^{-1})				
	0.1	0.5	1	5	10
FeO (kg)	5878	5356	5234	5090	5063
Carbon (kg)	210.6 (24.02 %)	70.6 (8.05 %)	40.8 (4.65 %)	10.2 (1.16 %)	5.3 (0.60 %)

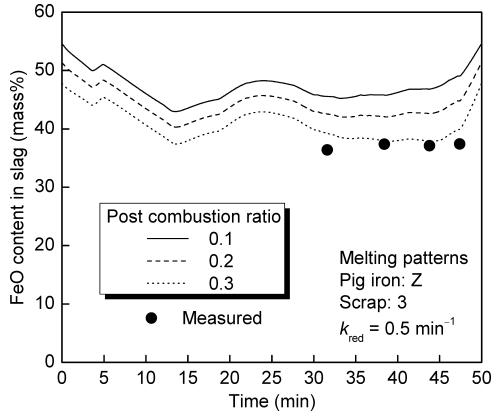

Fig. 6. Change of FeO content in slag with changing post combustion ratio.

The post combustion ratio just above the melt is around 0.1[6] and the computed optimized post combustion ratio of 0.3 is considered to be overestimated. As mentioned before, it was assumed that 20% of the injected oxygen through the post combustion injectors participates in the decarburization and oxidation reactions occurring in the melt and slag. When the contribution of the post combustion injector oxygen is decreased, the amount of FeO is also decreased resulting a decrease of the FeO in the slag.

4. Discussion

The model developed depends on a number of inputs including melting rates and reduction rate constants. The optimized set of parameters, which closely match the operational results are given in **Table 4**. The pig iron melting pattern is an important factor, while scrap melting is less important. Parameters in this table were obtained from above discussion, where one parameter was optimized with fixed other parameters. The complete optimization of parameters needs many heat data together with the proper optimization tool such as a sequential quadratic programming (SQP) algorithm. For instance, the SQP optimization is conducted with the objective function expressed as Eq. (25) to minimize the differences between the predicted values by the model and the operational results.

$$\sum_i |(P)_i^{\text{model}} - (P)_i^{\text{data}}| \times \rho_i \quad \text{.....(25)}$$

where, $(P)_i$ is $[\%C]^{\text{metal}}$ or $(\%MeO_n)^{\text{slag}}$ (Me=Fe, Ca, Si, Mg, *etc.*). Superscripts "model" and "data" represent the predicted value by the model and the operational result, respectively. ρ_i is the weight for species i resulting in different priority for the parameter optimization.

In general, the model over predicted the carbon content compared to the measured by about 0.1 %. The assumed decarburization rate constant may be larger than extrapolated from OSM. It was assumed that the rate decreased due to the lower oxygen flow rates. The effect of decarburization rate on the carbon content in the metal is shown in **Fig. 7**. The final carbon content in the melt and the final FeO content in the slag decreases from 0.037 to 0.018 mass% and from 47.5 to 48.0 mass%. The proper decarburization rate constant for each furnace can be obtained from the operation results of many heats.

The model can be used to optimize several aspects of the process. As will be presented in the next part of this paper, slag foaming can be optimized by controlling the FeO content, slag basicity and CO generation. Also nitrogen removal can be improved by changing the operation.

The model can be used to optimize yield. Yield can be improved by reducing the amount of FeO in the slag. This can be done by using carbon injection more effectively. Using more reactive forms of carbon will lower the FeO in the slag. The FeO content can also be lowered by reducing the oxygen flow rate at appropriate times during the melting cycle. Simulated case studies have been conducted, which indicate potential yield increases by changing these operational parameters. A 5% decrease of the oxygen flow rate (Case 1), 5% increase of the amount of carbon injected (Case 2), or an increase of the carbon–FeO reaction rate constant to 1.5 min^{-1}, simulating a more reactive form of carbon (Case 3), were applied while other operational parameters were fixed. **Table 5** shows the parameters applied and the summary of calculated results. In this paper, yield is calculated based on the iron (Fe) input into a furnace not the total scrap and pig iron. **Figure 8** shows the change of the carbon content in the metal and the FeO content in the slag with time for each case. The final carbon content in the metal increases by 0.005 mass% with the decreased oxygen flow rate (Case 1), while the carbon content does not change much in other cases. On the other hand, the final FeO content in the slag and the FeO loss with slag discharge decreases greatly, thus improving the yield by 0.12 to 0.76%.

In this model, the iron loss as dust is neglected. The dust produced is between 9 and 18 kg/t-scrap and contains around 50 mass% of iron oxide.[5,7] Therefore, the iron loss is considered to be more than that calculated in the present model, though the difference is small. Therefore, the actual yield would be slightly lower (0.2–0.5%) than calculated.

Yield is one aspect of the operation that should be considered together with the proper physical and chemical slag properties required for refining of the metal to remove im-

Table 4. The optimized set of parameters and the calculated results.

Melting patterns		R_{PC}	k_{red} (min^{-1})	%C final	%FeO final	FeO loss (kg)	Fe yield (%)
Pig iron	Scrap						
Z	3	0.3	0.57	0.037	47.5	4353	96.47

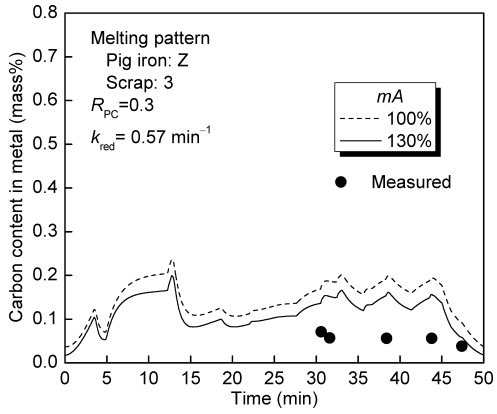

Fig. 7. Change of carbon content in metal with changing decarburization rate constant.

Table 5. Case study for yield improvement and the calculated result.

	Base Case	Case 1	Case 2	Case 3
Melting patterns	Pig iron: Z, Scrap: 3			
mA/V^{Oxy}	0.050			
R_{PC} (-)	0.3			
Oxygen injection	4212 Nm^3 Rate varies in process	5% decrease at 13-50 min	-	-
Coke injection	877 kg (20.5-50.0 min)	-	5% increase	-
k_{red} (min^{-1})	0.57	-	-	1.5
$[\%C]^{final}$	0.037	0.042	0.037	0.037
$(\%FeO)^{final}$	47.5	43.2	46.9	45.4
FeO loss (kg)	4353	3805	4271	4123
Fe Yield (%)	96.47	97.23	96.59	96.80

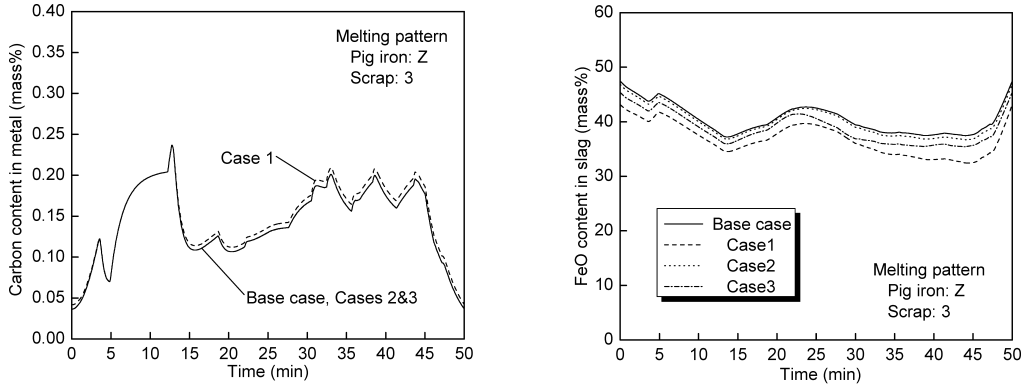

Fig. 8. Calculated results of (a) carbon content in metal and (b) FeO content in slag for each case.

purities and for effective slag foaming behavior. These additional points of consideration will be the subject of a future paper. The heat balance in the furnace should also be considered. For instance, the FeO loss and the yield are improved much in Case 1. However, the heat generated from the oxidation of iron must be compensated for with additional electrical input or a loss in overall productivity will result. The model developed in the present work will be utilized to optimize these inputs and outputs including the yield and the overall production cost.

5. Conclusions

In the present study, a decarburization and slag formation model for the electric arc furnace was developed. The model considers the rate phenomena for the decarburization and the carbon–FeO reaction in the slag, mass balance for each element in the metal, slag and gas phases, as well as the melting behavior of pig iron, scrap and fluxes. The model developed was applied to a two bucket charge operation furnace and the change of melt and slag compositions was calculated based on the operating conditions and compared to the operational results. The model can be used to predict iron yield and carbon loss with the discharged slag. It was determined that the pig iron melting pattern is very important in determining the carbon content in the melt. The change of FeO content in slag is affected by pig iron melting pattern, as well as the carbon–FeO reaction rate constant and post combustion ratio. The accurate input of operating parameters, such as the amount and compositions of charged raw materials and the initial heel, are required to simulate the operation. In addition, the optimization of melting patterns for pig iron, scrap and fluxes, carbon–FeO reaction rate constant and the post combustion ratio should be conducted through the comparison of calculated results with the real data for many heats.

Acknowledgements

Financial support and technical input from the member companies of the Center for Iron and Steelmaking Research in Carnegie Mellon University are gratefully acknowledged. Development and validation of the model with actual operational data from commercial electric arc furnaces, was made possible through the direct participation in this project by Gerdau. The authors also appreciate Dr. Il Sohn in U.S. Steel Research and Technology Center for the discussion about the model development.

Nomenclature

$[\%C]_t$: Carbon content in metal at time$=t$ (mass%)
$[\%C]_t^e$: Equilibrium carbon content in metal at time$=t$ (mass%)
$[\%C]^C$: Critical carbon content in metal (mass%)
$(\%MeO_n)_t$: Oxide MeO_n content in slag at time$=t$ (mass%)
k_{red}: Reduction rate constant of FeO by carbon in slag (min^{-1})
m: Liquid phase mass transfer coefficient of carbon (m/min)
r_t^{CM}: Reaction rate of carbonaceous material at time$=t$ (kg/min)
r_t^{Dirt}: Dissolution rate of dirt at time$=t$ (kg/min)
r_t^{Dis}: Slag discharge rate at time$=t$ (kg/min)
r_t^{Flux}: Dissolution rate of flux at time$=t$ (kg/min)
r_t^{Pig}: Melting rate of pig iron at time$=t$ (kg/min)
r_t^{red}: Reduction rate of FeO by carbon in slag (kg/min)
r_t^{Scrap}: Melting rate of scrap at time$=t$ (kg/min)
t: Time (min)
A: Interfacial area for the decarburization reaction (m^2)
$C_{CM}^{MeO_n}$: Content of oxide MeO_n in carbonaceous material (−)
$C_{Dirt}^{MeO_n}$: Content of oxide MeO_n in dirt (−)
$C_{Flux}^{MeO_n}$: Content of oxide MeO_n in flux (−)
C_{Pig}^{Me}: Content of element Me in pig iron (−)
C_{Scrap}^{Me}: Content of element Me in scrap (−)
$C_t^{MeO_n}$: Content of oxide MeO_n in slag phase at time$=t$ (−)
R_{PC}: Post combustion ratio (−)
V_t^{Oxy}: Oxygen gas injection rate at time$=t$ (m^3/min)
W_t^{CM}: Weight of carbonaceous materials existing in slag phase at time$=t$ (kg)
$W_t^{Fe\text{-}Red}$: Weight of reduced iron in slag phase at time$=t$ (kg)
W_t^{Melt}: Weight of metal phase at time$=t$ (kg)
W_t^{Me}: Weight of element Me in metal phase at time$=t$ (kg)

$W_t^{MeO_n}$: Weight of oxide MeO_n in slag phase at time$=t$ (kg)
$W_t^{Me\text{-}Oxi}$: Weight of oxidized element Me at time$=t$ (kg)
W_t^{Slag}: Weight of slag phase at time$=t$ (kg)
Δt: Calculation time step (min)
ρ: Density of melt ($=7\,200$) (kg/m^3)

REFERENCES

1) R. J. Fruehan (ed.): The Making, Shaping and Treating of Steel, 11th ed., The AISE Steel Foundation, Pittsburgh, PA, (1998), 525.
2) R. J. Fruehan (ed.): The Making, Shaping and Treating of Steel, 11th ed., The AISE Steel Foundation, Pittsburgh, PA, (1998), 475.
3) R. J. Fruehan (ed.): The Making, Shaping and Treating of Steel, 11th ed., The AISE Steel Foundation, Pittsburgh, PA, (1998), 124.
4) B. Deo and R. Boom: Fundamentals of Steelmaking Metallurgy, Prentice Hall International, Hemel Hempstead, UK, (1993), 194.
5) R. Fortes: private communication.
6) R. J. Fruehan (ed.): The Making, Shaping and Treating of Steel, 11th ed., The AISE Steel Foundation, Pittsburgh, PA, (1998), 611.
7) R. J. Fruehan (ed.): The Making, Shaping and Treating of Steel, 11th ed., The AISE Steel Foundation, Pittsburgh, PA, (1998), 590.